

# Residual Stress Analysis of Aluminum-doped Zinc Oxide Films under Laser-Induced Recovery Process

Yu-Chen Hsieh, Ching-Ching Yang, Chih-Chung Yang, Yu-Hsuan Lin, Kuo-Cheng Huang  
and Wen-Tse Hsiao

*Instrument Technology Research Center, National Applied Research Laboratories, 20, R&D Rd. VI, Hsinchu Science Park,  
Hsinchu City, Taiwan*

**Keywords:** Ultraviolet Laser System, Low-temperature Annealing, Aluminum Doped Zinc Oxide Films, Induced-crystalline, Residual Stress Analysis.

**Abstract:** In this study, a low-temperature annealing technique using an ultraviolet laser was proposed for inducing the crystallization of transparent conductive aluminum-doped zinc oxide (AZO) films. The technique was used in conjunction with a galvanometer scanner to adjust the laser energy density and scanning speed, thereby inducing the amorphous crystallization of thin films. X-ray diffraction was used to analyze the structural properties of annealed thin films. Analysis with different galvanometer scanning speed during annealing and laser pulse repetition rates during annealing revealed that the two diffraction peaks (i.e., the (002) and (103) peaks) of the zinc oxide thin films became more noticeable as the laser pulse repetition rate increased. When the galvanometer scanning speed during annealing was set to 400 mm/s and 600 mm/s, the full width at half of the maximum (FWHM) of the AZO thin films decreased while the annealing frequency increased. By contrast, when the annealing speed was 800 mm/s, increasing the annealing frequency caused the FWHM to decrease and then increase. An analysis of the residual stress of the annealed thin film confirmed that when the annealing speed was reduced from 800 mm/s to 400 mm/s, increases in laser pulse repetition rate resulted in increased residual stress.

## 1 INTRODUCTION

Regarding the development of materials and techniques used in manufacturing monitors, the three major materials used for creating thin-film-transistor (TFT) components are amorphous-silicon (a-Si) thin films, poly-silicon thin films, and oxide semiconductors. To meet the requirements of the wearable-device and Internet of Things industries, optoelectronic components should be light, thin, short, and multifunctional. Additionally, in response to the advocacy for energy-efficient policies, highly efficient components with low power consumption have become increasingly prevalent in electronic products. The resistivity, crystallization (i.e., amorphous, crystalline, and polycrystalline), carrier concentration, and electron mobility of transparent conductive thin-film materials can affect the efficiency and power consumption of a thin-film device. Recrystallization annealing can be used to address problems concerning the electron mobility and off-state current of conventional a-Si TFTs.

Conventional methods for changing the crystalline state of an amorphous thin film include solid-phase crystallization, metal-induced crystallization, and excimer laser crystallization. (Coherent, Inc. 2015) proposed a technique involving the use of excimer lasers to perform low-temperature a-Si laser annealing. This technique can increase monitor resolution and is applicable to large-scale monitors, active-matrix liquid-crystal displays, active-matrix organic light-emitting diodes, organic light-emitting diode televisions, and flexible electronics. (Zhang et al. 2012) applied nanosecond and picosecond single-shot lasers to induce the crystallization of  $\text{Ge}_2\text{Sb}_2\text{Te}_5$  thin films and plot a curve representing the relationship between crystallization temperature and instantaneous laser energy. This enabled examination of the ablation threshold, melt threshold, solid-phase crystallization, and melt recrystallization of thin films. Their experimental results confirmed that recrystallization could be achieved under the ablation threshold of  $\text{Ge}_2\text{Sb}_2\text{Te}_5$  by using different values of laser energy density and exposure time to improve the

characteristics of the material. (Huang et al. 2013) used relevant theories to conduct an experiment in which a-Si thin films were exposed to a green-light nanosecond laser at 532 nm; subsequently, a finite element analysis was conducted to simulate the melt-recrystallization process and determine the optimal energy density. Their experimental results revealed that the recrystallization temperature and melting depth varied with the laser exposure time. Specifically, the results of Raman spectroscopy revealed that the optimal crystallization was achieved when the energy density was 1000 mJ/cm<sup>2</sup>. By using excimer lasers to induce the recrystallization of a-Si/SiO<sub>2</sub>/glass thin films, (Kuo et al. 2007) investigated the effect of excimer laser during the melting process on silicon recrystallization, film thickness, and substrate temperature. They observed notable changes in film thickness when the melting duration was increased, particularly at high temperatures. (Emelyanov et al. 2014) used femtosecond lasers to induce the recrystallization of a-Si thin films; specifically, the experiment involved adjusting the energy density of the laser to identify the parameters affecting the structure and photoelectrical characteristics of such thin films. (Cheng et al. 2014) used a high-repetition-rate femtosecond laser to induce the crystallization of transparent conductive thin films composed of amorphous indium tin oxide (ITO). The results revealed that with the laser energy of 536 mJ, repetition rate of 0.05 MHz, and scanning speed of 0.25 mm/s, the crystal structure was perpendicular to the scanning path (E/C). (Lee et al. 2010) used a 248-nm krypton fluoride excimer laser to anneal aluminum-doped zinc oxide (AZO) thin films and analyze their structure, surface morphology, and photoelectrical characteristics. The laser energy density and frequency were fixed at 160 mJ/cm<sup>2</sup> and 10 Hz, respectively, and the laser pulse number ranged between 600 and 3000. The scanning electron microscopic analysis revealed that during the laser annealing process, the pore size of the thin film was reduced, thereby increasing the grain boundary. The XRD analysis confirmed that when the number of laser pulses increased, the diffraction peak intensity also increased, indicating more favorable crystalline characteristics. (Tsang et al. 2008) adopted the sol-gel process to prepare AZO thin films, and a krypton fluoride excimer laser was used at various energy levels to anneal the thin films. The XRD analysis revealed that under a fixed laser pulse number, increasing the laser energy caused the diffraction peak values to increase. Similarly, increasing the laser pulse number under fixed laser energy also increased

the diffraction peak values, indicating that both laser energy and pulse number affected the thin-film structure. Investigations of the electrical characteristics of annealed crystalline structures have revealed that resistivity noticeably decreases in response to increases in laser energy. This phenomenon is attributable to the increased electron mobility caused by crystal defects and reduced grain boundary density (Tsang et al. 2008). (Chen et al. 2012) (Chen et al. 2011) used laser beam shaping techniques to anneal transparent conductive ITO thin films and fluorine-doped tin oxide thin films. Their results revealed that laser processing parameters (e.g., spot shape, energy distribution, spot overlay, and operating modes) affected the photoelectrical characteristics of annealed thin films. In the case of the fluorine-doped tin oxide thin film, its resistivity decreased from  $7.19 \pm 0.55$  to  $6.70 \pm 0.20 \times 10^{-3}$  Ω-cm. (Kim et al. 2011) proposed a low-cost annealing technique applicable to large-scale metal-oxide thin films that could be used to manufacture TFT liquid-crystal displays and flexible electronics. They noted that conventional annealing chambers require an annealing temperature of >400 °C, which is unsuitable for processing the substrates of flexible electronics; hence, they proposed a low-temperature manufacturing technique (<200 °C) to anneal four thin-film materials (In<sub>2</sub>O<sub>3</sub>, a-Zn-Sn-O, a-In-Zn-O, and ITO). (Morimoto et al. 2012) used a 405-nm gallium nitride laser diode as the light source for inducing the crystallization of a-Si TFTs, which were compared with those with crystallization induced with commercially available 405-nm, 445-nm, and 532-nm light sources. The results confirmed that a-Si exhibited a greater absorbance coefficient at 405 nm. Data from the simulation and experiment regarding the evenness of the resulting crystalline structure and efficiency of the crystallization process indicated that the proposed method can be used to recrystallize and transform a-Si into micro crystalline Si. (Huang et al. 2016) proposed a 532 nm pulse laser to anneal Al-doped ZnO films on polyethylene terephthalate (PET) flexible substrate. By using the laser annealing could greatly enhance grain crystalline. When the crystalline size increased and avoid damage to the PET flexible substrates. (Xu et al. 2018) used light emission based physical approaches to measure the driving voltage, reverse current versus relative light intensity. In addition, the spectroscopic information shown that the electroluminescence (EL) spectrum has a broad emitting range of 400-900 nm.

## 2 THE PROPOSED LASER-INDUCED RECOVERY SYSTEM, SAMPLE PREPARED, AND RESIDUAL STRESS ANALYSIS

The proposed low-temperature laser annealing system contains a Nd:YVO<sub>4</sub> laser source, galvanometer scanning module, and beam delivery system. The specifications of the proposed system are as follows: a laser wavelength of 355 nm, maximal output power of 14 W, spatial mode of TEM<sub>00</sub>, maximal pulse repetition rate of 300 kHz, and pulse width of 30 ns. The galvanometer scanning module consists of a telecentric lens with a focal length of 163 mm, and its scanning range reaches 60 mm × 60 mm, which is sufficient for covering the entire annealing area. The transparent conductive AZO thin film was prepared first by using a sputtering approach to deposit the film on a Corning Eagle 2000 glass substrate (Corning Inc., United States) with an approximate thickness of 200 nm. To avoid damaging the glass substrate during the annealing process, the laser energy was maintained at 61.2 μJ, while the pulse repetition rate was adjusted to 40, 55, and 70 kHz and the scanning speed was adjusted to 400, 600, and 800 mm/s. In Bragg's law (1), *d* denotes lattice spacing, *θ* denotes diffraction angle, and *λ* denotes X-ray wavelength (0.154 nm). Accordingly, *d* decreases when *θ* increases, indicating a decrease in film stress. Therefore, a biaxial stress model can be used to estimate the residual stress of a thin film during modification (Jun et al. 2012). Film stress can be estimated using (2) when it is being analyzed in the *c*-axis direction using XRD.

$$2d \sin \theta = n\lambda \quad (1)$$

$$\varepsilon_{film} = \frac{C_{film} - C_{bulk}}{C_{bulk}} \quad (2)$$

where *C<sub>bulk</sub>* is the lattice strain constant (0.2609 nm) of the ZnO thin film. *C<sub>film</sub>* was estimated by substituting the lattice parameter of the AZO thin film that was derived from XRD analysis into (1). The surface-layer stress of the thin film can be estimated using (3) (Jo et al. 2018).

$$\sigma_f = \frac{2c_{13}^2 - c_{33}(c_{11} + c_{12})}{2c_{13}} \times \varepsilon_{film} \quad (3)$$

where *c<sub>ij</sub>* is the elastic constant of ZnO. According to research on elastic constants (Cebulla et al. 1998), *c<sub>11</sub>* = 208.8 GPa, *c<sub>12</sub>* = 119.7 GPa, *c<sub>13</sub>* = 104.2 GPa, and *c<sub>33</sub>* = 213.8 GPa.

## 3 STRUCTURE ANALYSIS OF ANNEALED AZO THIN FILMS

Figure 1 presents the XRD spectra of the AZO thin films deposited on a Corning Eagle 2000 glass substrate at different galvanometer scanning speed during annealing and laser pulse repetition rates (40, 55, and 70 kHz). The spectra exhibited two noticeable diffraction peaks of the zinc oxide thin films, namely the (002) and (103) peaks. Increasing the laser pulse repetition rate caused a substantial increase in the intensity of the (002) peak. The Scherrer equation is used for calculating the crystallite size from FWHM of the (002) peak.

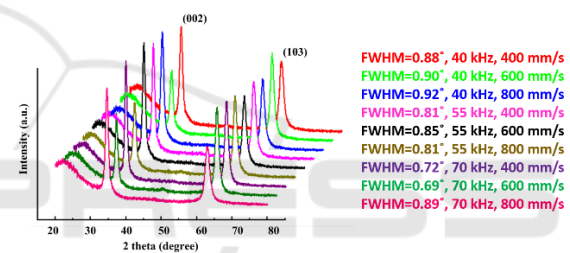


Figure 1: XRD spectrum of AZO films under different recovery process conditions. (Hsiao et al. 2013).

As indicated in Figure 2, when the galvanometer scanning speed during annealing was set to 400 and 600 mm/s, the FWHM of the annealed AZO thin film decreased in accordance with the increasing annealing frequency. When the galvanometer scanning speed during annealing was set to 800 mm/s, the increase in annealing frequency caused the FWHM to decrease and then increase. These findings indicated that the grain size of the annealed thin film was affected by the laser pulse repetition rate and scanning speed.

The results displayed in Figure 3 revealed that when the galvanometer scanning speed during annealing was reduced from 800 to 400 mm/s, the grain size increased from 7.4 nm to 12 nm. Figure 4 presents the residual stress of the annealed AZO thin films under the laser pulse repetition rates of 40, 55, and 70 kHz and scanning speeds of 400, 600, and 800 mm/s; residual stress was calculated using (1)–(3). The results confirmed that the residual stress of the thin films increased in accordance with increases in the laser pulse repetition rate. By contrast, the

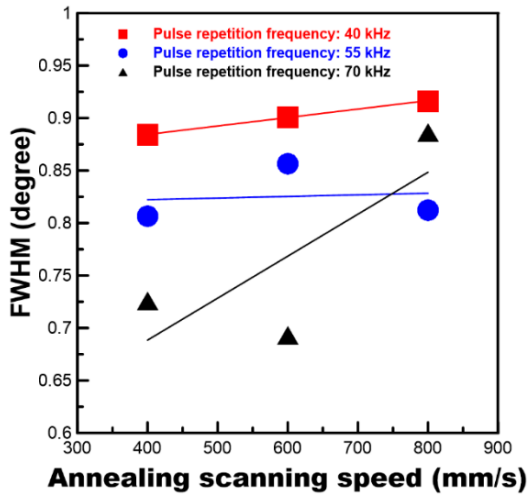


Figure 2: Relationship between FWHM versus different annealing speeds.

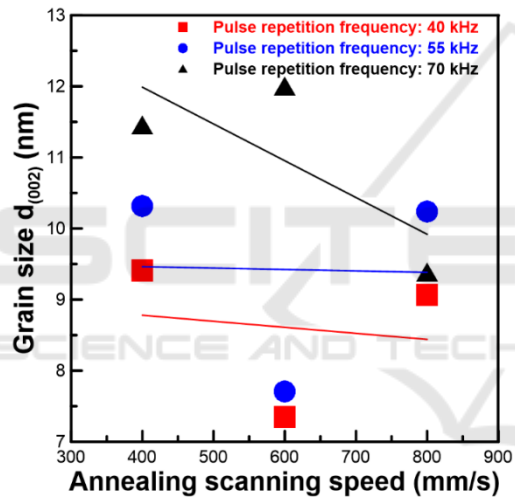


Figure 3: Grain size versus annealing speeds under different pulse repetition frequency.

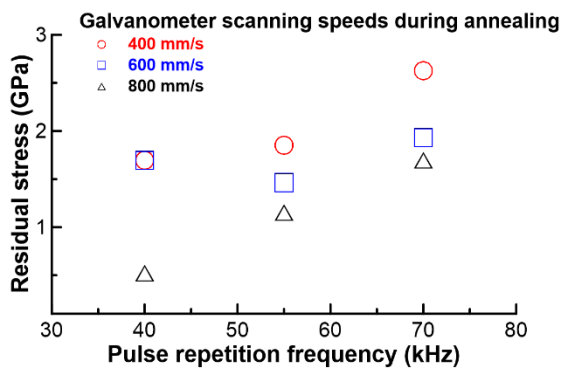


Figure 4: Residual stress versus pulse repetition frequency under different speeds.

residual stress decreased with increasing scanning speeds under a constant laser pulse repetition rate. This was attributable to both the increases in pulse energy of the Nd:YVO<sub>4</sub> laser source in accordance with the increasing repetition rate and the accumulation of excessive heat on the thin-film surface as a result of a low scanning speed.

## 4 CONCLUSIONS

A low-temperature annealing technique using an ultraviolet laser was proposed in this study for inducing the crystallization of transparent conductive AZO thin films. XRD was used to analyze the structure of annealed thin films. The resulting XRD spectra exhibited two noticeable diffraction peaks, (002) and (103), the intensity of which increased with an increasing laser pulse repetition rate. The FWHM of the AZO thin film increased in accordance with decreasing annealing frequency. When the galvanometer scanning speed during annealing was 800 mm/s, increasing the annealing frequency caused the FWHM to decrease and then increase. When the scanning speed during annealing was reduced from 800 to 400 mm/s, increasing the laser pulse repetition rate increased the residual stress of the thin film. Under a fixed laser pulse repetition rate, the residual stress of the thin film decreased with the increasing scanning speed during annealing. This was attributable to two phenomena: the pulse energy of the Nd:YVO<sub>4</sub> laser source increased as a result of an increasing repetition rate, and excessive heat accumulated on the thin-film surface because of the low scanning speed. Table 1 summarizes the stress under different annealing processes of AZO films (Jo et al. 2018) (Huang et al. 2016) and (Kim et al. 2017). In this experiment results indicated that the calculated the stress values in the annealed AZO films were approximately less than 3 GPa. During the higher scanning speed of 800 mm/s, the residual stress were less than 2 GPa.

Table 1: Specification of the picosecond laser scanning system.

Authors	Methods	Stress (GPa)
(Jo et al. 2018)	UV +RTA	-0.3 ~ 0.7
(Huang et al. 2016)	Green laser	-
(Kim et al. 2017)	UV + RTA	-
Our present	UV laser	< 3

## ACKNOWLEDGEMENTS

This work was supported in part by the Ministry of Science and Technology, TAIWAN, numbers MOST 106-2221-E-492 -012 and 107-2622-E-492 -009 -CC3

## REFERENCES

- COHERENT, Co. Ltd., 2015. White paper: The digital display revolution: Built on Excimer laser annealing.
- Zhang, K., Li, S., Liang, G., Huang, H., Wang, Y., Lai, T., Wu, Y., 2012. Different crystallization processes of as-deposited amorphous Ge<sub>2</sub>Sb<sub>2</sub>Te<sub>5</sub> films on nano- and picosecond single laser pulse irradiation. *Physica B*, Vol. 407, pp. 2447-2450.
- Huang, L., Jina, J., Shia, W., Yuanb, Z., Yanga, W., Caoa, Z., Wang, L., Zhou, J., Loub, Q., 2013. Characterization and simulation analysis of laser-induced crystallization of amorphous silicon thin films. *Mater. Sci. Semicond. Process.* Vol. 16, pp. 1982-1987.
- Kuo, C.C., Yeh, W.C., Lee, J.F., Jeng, J.Y., 2007. Effects of Si film thickness and substrate temperature on melt duration observed in excimer laser-induced crystallization of amorphous Si thin films using in-situ transient reflectivity measurements. *Thin Solid Films* Vol. 515, pp. 8094-8100.
- Emelyanov, A.V., Khenkin, M.V., Kazanskii, A.G., Forsh, P.A., Kashkarov, P.K., Gecevicius, M., Beresna, M., Kazansky, P.G., 2014. Femtosecond laser induced crystallization of hydrogenated amorphous silicon for photovoltaic applications. *Thin Solid Films* Vol. 556, pp. 410-413.
- Cheng, C.W., Lee, I.M., Chen, J.S., 2014. Femtosecond laser-induced nanoporous structures and simultaneous crystallization in amorphous indium-tin-oxide thin films. *Appl. Surf. Sci.* Vol. 316, pp. 9-14.
- Lee, S., Seong, J., Kim, D.Y., 2010. Effects of laser-annealing using a KrF excimer laser on the surface, structural, optical, and electrical properties of AlZnO thin films. *J. Korean Phys. Soc.* Vol. 56, pp. 782-786.
- Tsang, W.M., Wong, F.L., Fung, M.K., Chang, J.C., Lee, C.S., Lee, S.T., 2008. Transparent conducting aluminum-doped zinc oxide thin films prepared by sol-gel process followed by laser irradiation treatment. *Thin Solid Films* Vol. 517, pp. 891-895.
- Chen, M.F., Lin, K.M., Ho, Y.S., 2012. Laser annealing process of ITO thin films using beam shaping technology. *Opt. Lasers Eng.* Vol. 50 pp. 491-495.
- Chen, M.F., Lin, K.M., Ho, Y.S., 2011. Effects of laser-induced recovery process on conductive property of SnO<sub>2</sub>:F thin films. *Mater. Sci. Eng. B* Vol. 176, pp. 127-131.
- Kim, M.G., Kanatzidis, M.G., Facchetti, A., Marks, T.J., 2011. Low-temperature fabrication of high-performance metal oxide thin-film electronics via combustion processing. *Nat. Mater.* Vol. 10, pp. 382-388.
- Morimoto, K., Suzuki, N., Liu, X., Samonji, K., Yamanaka, K., Yuri, M., 2012. Amorphous Si crystallization by 405 nm GaN laser diodes for high performance TFT applications: advantages of using 405 nm wavelength. *Proc. of SPIE* Vol. 8244, pp. 824407-1.
- Jun, M.C., Park, S.U., Koh, J.H., 2012. Comparative analysis of Al-doped ZnO and Ga-doped ZnO thin films. *Integr. Ferroelectr.*, Vol. 140, pp. 166-176.
- Cebulla, R., Wendt, R., Ellmer, K., 1998. Al-doped zinc oxide films deposited by simultaneous rf and dc excitation of a magnetron plasma: relationships between plasma parameters and structural and electrical film properties. *J. Appl. Phys.* Vol. 83, pp. 1087-1095.
- Hsiao, W.T., Tseng, S.F., Huang, K.C., Chiang, D., 2013. Electrode patterning and annealing processes of aluminum-doped zinc oxide thin films using a UV laser system. *Opt. Laser Eng.* Vol. 51, pp. 15-22.
- Huang, L.J., Li, B.J., Ren, N.F., 2016. Enhancing optical and electrical properties of Al-doped ZnO coated polyethylene terephthalate substrates by laser annealing using overlap rate controlling strategy. *Ceramic International* Vol. 42, pp. 7246-7252.
- Jo, G.H., Kim, S.H., Koh, J.H., 2018. Enhanced electrical and optical properties based on stress reduced graded structure of Al-doped ZnO thin films. *Ceramic International* Vol. 44, 735-741.
- Xu, K., Huang, L., Zhang, Z., Zhao, J., Zhang, Z., Snyman, L.W., Swart, J.W., 2018. Light emission from a polysilicon device with carrier injection engineering. *Materials Science & Engineering B* Vol. 231, pp. 28-31.
- Kim, J., Ji, J.H., Min, S.W., Jo, G.H., Jung, M.W., Park, M.J., Lee, S.K., Koh, J.H., 2017. Enhanced conductance properties of UV laser / RTA annealed Al-doped ZnO thin films. *Ceramic International* Vol. 43, 3900-3904.